Discover Electronics

Perspective

Future prospects of 6G wireless communication: review of antenna technologies

Ameelia Roseline A[1] · **Pranav Mohan Kumar**[2]

Received: 29 July 2024 / Accepted: 12 December 2024
Published online: 24 December 2024

Abstract
The sixth generation (6G) wireless technology is designed for advanced applications such as immersive reality, autonomous vehicle communication, and holographic communication. Central to 6G systems are RF transceivers, including amplifiers, mixers, and antennas. For 6G to support higher data rates and ensure network reliability in higher frequency bands, antennas need to be simple in design, cost-effective for mass production, and have better radiation performance than 5G antennas. This paper provides a brief review of recent advancements in 6G antenna design, covering deployment scenarios, design methodologies, and radiation characteristics, aiming to enhance readers' understanding of 6G antenna architectures.

Keywords 6G wireless technology · Antenna applications · MIMO antenna · Extended virtual reality

1 Introduction

Early in the 2030s is when sixth generation (6G) wireless technology is anticipated to become a reality. [1, 2].To make this technology a reality, engineers, governments, international bodies are actively investing in research to make this promise a reality. Although the 6G technology is built on the foundation of fifth generation (5G) and 5G advanced, 6G technology is expected to provide a higher spectral efficiency, very low latency, optimal AI (Artificial Intelligence) and ML (Machine Learning) connectivity, and higher data coverage than 5G. Some notable applications include extended virtual reality (XR), digital twins, and holographic communications. Essentially, it is anticipated that 6G technology would close the gap between the digital and real worlds. To support these applications, you need enabling technologies such as Reconfigurable Intelligent Surfaces (RIS), AI, Non-Terrestrial Networks (NTNs), ultra massive MIMO and more. The main challenge for WPT is the sharp decline in energy transfer efficiency with distance due to considerable route loss. Researchers have examined MIMO systems, especially massive MIMO, and energy beamforming algorithms for their ability to direct highly directed RF signal power onto user equipment (UEs) in order to address this problem [3–6]. Fading may have a substantial influence on wearable device-to-wearer communication in practical wireless propagation circumstances, especially where wireless communication is essential for military operations team coordination, mission control, and situational awareness [7]. It is now simple and quick to design microstrip filters using a Transmission Line model (TL) and Genetic Algorithm (GA). To demonstrate the effectiveness of the recommended approach, a wideband second-order bandpass filter with a center frequency of 2.3 GHz

✉ Ameelia Roseline A, ameeliaroseline@gmail.com; Pranav Mohan Kumar, pranavus94@gmail.com | [1]Department of Electronics and Communication Engineering, Panimalar Engineering College, Chennai, Tamilnadu, India. [2]The Math Works Inc., 1 Lakeside Campus Drive, Natick MA-01760, USA.

is tested using two short-circuited and two open-circuited stubs [8]. In recent years, off-chip DRA designs, such as small and in-substrate DRAs, have become more and more popular. The reason behind this increase in demand is the swift advancement of economical methods for producing multilayer laminates, like Low-Temperature Co-fired Ceramic (LTCC) and Printed Circuit Boards (PCBs) [9]. Regardless of the application 6G supports, RF (Radio Frequency) transceivers are inevitable part of a 6G architecture. A generic RF MIMO (Multiple-Input Multiple-Output) transceiver is shown in the Fig. 1. This generic RF MIMO transceiver architecture included a phase shifter at its transmitter and its receiver. This is because to accurately capture the transmitted signal, phase shifts are necessary to align the array beam with the direction from which the received signal arrives [10]. It should be noted that the input to the RF transmitter and the output from the RF receiver are not depicted in Fig. 1, as the main emphasis of this review paper is on antenna designs rather than RF transceiver architectures.

This paper focusses on a review of the around 50 most promising 6G antenna architectures, a key component of RF transceivers. This paper also highlights the key characteristics of these antenna architectures and how it can be a considered a promising candidate for 6G applications. The 6G antenna architectures are sorted based on their operating frequencies: mid- and high-frequency band antennas. Mid-frequency band 6G antennas operate between 1–100 GHz and high-frequency band 6G antennas operate above 100 GHz. This paper also provides antenna overview tables that highlights key characteristics of the antennas that are discussed in this review paper. The antennas are reviewed or succinctly summarized based on increasing order of resonant frequencies.

The remainder of the work is structured in this manner. In each of the sections 2 and 3, which provide a brief summary of the features and performance of each design, a brief discussion of the relative benefits and drawbacks of each antenna type as well as comparisons with the results of current technologies would give readers a more nuanced understanding of their practical implications. Section 2 summarizes the key characteristics of mid-frequency 6G antennas, while Section 3 summarizes the key characteristics of high-frequency 6G antennas as documented in recent publications. The developed results in this review work can be studied in a number of ways; these are briefly described in Section 4 as potential future directions. Finally, we conclude the paper in Section 5.

Table 1 in section 2 and Table 2 in section 3 offers a comprehensive overview of the essential features of mid-frequency and high frequency 6G antennas as outlined in recent scholarly publications respectively. Specifically, it presents a concise summary of 50 diverse antenna designs, detailing their operating frequencies and highlighting key characteristics. The tables also include important specifications such as bandwidth, gain, aperture efficiency, and S_{11}, which are critical for evaluating antenna performance. Table 3 in section 3 summarizes the fabrication technology, advantages, disadvantages, applications, and challenges of a few previous works. Table 4 in section 4 summarizes the various implementation methods and technologies for a few contemporary 6G wireless communication networks. By compiling this information in a single, easy-to-navigate format, Table 1, 2, 3 & 4 serves as a valuable quick reference for researchers. It enables them to efficiently compare and contrast the fundamental aspects of different antenna designs, facilitating informed decision-making in the exploration and development of 6G antenna technologies. This structured presentation of data not only saves time but also helps in identifying the most suitable antenna configurations for specific applications or research needs.

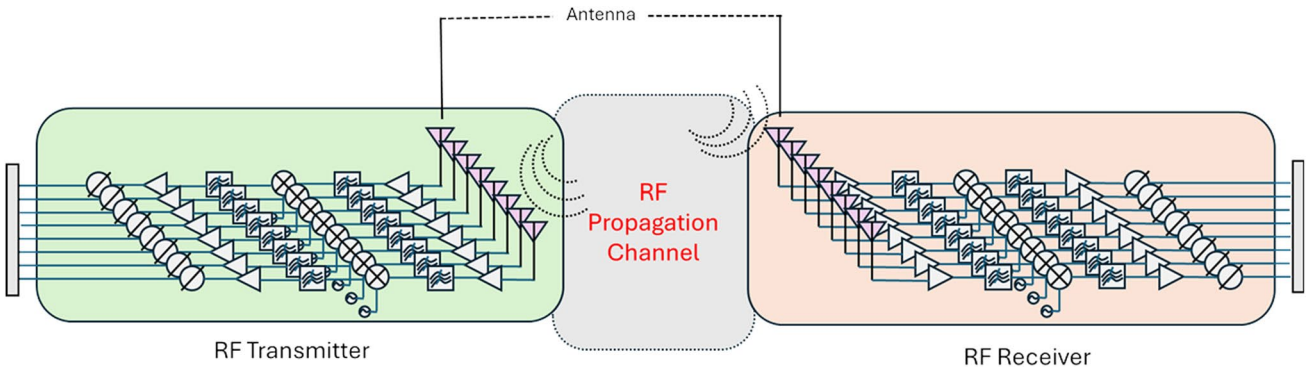

Fig. 1 Generic RF MIMO Transceiver

Table 1 Summary of the key characteristics of mid-frequency 6G antennas

Ref #	Antenna type	Resonant frequency	Key characteristics	Antenna specifications	Simulated using
[11]	8-Port MIMO antenna module	6.425 GHz	• Compact • High spectral efficiency (56 bps/Hz) • FR4 Substrate • Mobile telecommunication	Bandwidth = 6.425–7.125 GHz	Ansys HFSS full wave EM simulator
[12]	4-port MIMO antenna module	7.025 GHz	• Compact • High spectral efficiency (56 bps/Hz) • FR4 Substrate • Mobile telecommunication	Bandwidth = 7.025–8.4 GHz	Ansys HFSS full wave EM simulator
[19]	Planar lens antenna	10 GHz and 10.4 GHz	• Capacitive and Inductive features on a single layer • X-band applications • Rogers 4350 substrate • Single layer metasurface	Gain = 16.3 dBi at 10 GHz and 13.2 dBi at 10.4 GHz	Ansys HFSS full wave EM simulator
[20]	Glass shaped patch antenna	10.06 GHz, Wi-Fi, and 19.42 GHz	• Low-profile • Ultra wideband • FR4 substrate • Wi-Fi, 5G and 6G communications	• Operating band = 2.69 GHz–20.05 GHz • Gain = 2.2 dB at 10.06 GHz; 3.24 dB and 4.23 dB over Wi-Fi bands; 8.17 dB at 19.42 GHz • S11: − 26.94 dB at 3.76 GHz, − 22.96 dB at 8.89 GHz, − 22.59 dB at 11.59 GHz, − 22.71 dB at 17.09 GHz, and − 24.01 dB at 18.88 GHz • VSWR < 2 in the operating bandwidth	Ansys HFSS full wave EM simulator
[21]	64-by-64 slotted stacked patch antenna array	19.5 and 29.5 GHz	• Filtennas • Light-in-weight • Cost-effective • RO4003 substrate • K/Ka band Satellite mobile communication systems	• Operating band = 17.5 GHz–21.5 GHz/27.5 GHz–31.5 GHz • Gain = 7.8–9.22 dBi	ADS & Ansys HFSS full wave EM simulator
[22]	Sandwiched PRS (partially reflective surface) Fabry–Perot antenna	25.3 GHz	• Compact • High aperture efficiency • RO3010 and RT/Duroid 5880 • mm-wave	• Gain = 12.35 dBi at 25.3 GHz • Aperture efficiency = 79.4% • Cavity height = λ/17	Ansys HFSS full wave EM simulator
[23]	Wearable ring Metal-dielectric and DR antennas	28 GHz And 13.2 GHz	• Wearable • Low-cost • Fuse filament fabrications • Poly-lactic acid (PLA)/RT-Duroid 5880/ PREPERM® ABS1000 • 3-D Printing • mm-Wave	BW = 0.6 GHz Gain = 6 dB S_{11} = − 22 dB	CST Micro Wave Studio

Table 1 (continued)

Ref #	Antenna type	Resonant frequency	Key characteristics	Antenna specifications	Simulated using
[24]	Wideband, high-efficiency electromagnetic structure	60 GHz	• Antenna In package • Wideband • Common mode suppression • Rogers 3003 • 5G/6G Antenna-in-Package (AiP) applications	22% impedance bandwidth = 60–75 GHz, Relative Gain = 8–10 dBi 3-dB beamwidth: E-plane: 50° H-plane: 45°	Not specified
[25]	mm-wave Conical-beam antennas	76 GHz	• Conical radiation • Compact • Highly stable conical beam radiation • Duroid 5880 substrate • mm-wave, 6G LEO, E-band, V-band	• Gain = 12.05 dB • Operating band = 59.38–89.95 GHz; 40.9%	Not specified
[26]	Tooth-shaped patch antenna	77 GHz	• Lower mutual coupling effect with higher gain • Rogers RO/Duroid 5880 • mm-wave and Autonomous vehicle	Gain = 9.4 dB	Ansys HFSS full wave EM simulator

Table 2 Summary of the key characteristics of high frequency 6G antennas

Ref #	Antenna type	Resonant frequency/frequency range	Key characteristics	Antenna specifications	Simulated using
[27]	8-by-8 Antenna array module	110 GHz	• Compact • Low dielectric loss • Sub-THz	• Gain = 19.65 dBi • Bandwidth = 9.19 GHz	Ansys HFSS full wave EM simulator
[28]	SIW slot antenna	114.25, 134.75, 124, 144, 154, and 160 GHz	• Wideband • Six resonant frequencies • Rogers Duroid 5880 • D-band	Operating Bandwidth = 110–170 GHz	Ansys HFSS full wave EM simulator
[29]	Leaky-wave wire antenna	120 GHz	• Copper wire and Teflon rod • Simple • Low cost • Easy to fabricate • Copper wires twisted around Teflon rod • D-band	• Gain = 9.9 dBi • Operating band = 115 to 180 GHz	CST Microwave Studio
[30]	Stacked patch 4-by-4 antenna array	140 GHz	• Wide bandwidth • High gain • Economical • ASTRA MT77 Substrate • Multilayered standard PCB fabrication • D-band	• Gain = 16 dBi • Operating band = 123 to 158 GHz	Ansys HFSS full wave EM simulator
[31]	MIMO Antenna array	150 GHZ	• Simple • Wide band • High gain • D-band	• Gain = 18.3 dBi • Bandwidth = 142 to 155.5 GHz	Not specified
[32]	multi slot THz microstrip antenna	217 GHz and 228 GHz	• Simple • Miniaturization • Easy to fabricate • Silicon substrate • Terahertz 6G communication	• Operating bandwidth = 217 GHz-250 GHz • Gain = 3.7 dB and 4.5 dB	Ansys HFSS full wave EM simulator
[33]	CP Sub-THz four-layer antenna	285 GHz	• Low-profile • Circular polarized • Four-layer antenna • WR-3 waveguide • Sub-THz	• Gain = 11.9 dBic • Operating bandwidth = 270–295 GHz	Not specified
[34]	CP horn antenna	300 GHz	• Circular polarized • Compact • Electrical discharge machining • Brass • Wire-cutting EDM	• Gain = 18.3 dBic • 3 dB axial ratio bandwidth = 7 GHz(309 GHz-316 GHz) being 2.3% with a minimum axial ratio of 1.15 dB at 312 GHz • Total efficiency = 87.5% • Radiation efficiency = 99%	CST Microwave Studio

Table 2 (continued)

Ref #	Antenna type	Resonant frequency/frequency range	Key characteristics	Antenna specifications	Simulated using
[35]	THz dipole reflector antenna	310 GHz	• Half-circle-shaped directors • short-range THz communication • Compact • Benzo-Cyclo-Butene (BCB) • Broadband wireless high-data-rate communication	• Gain = 7.27 dBi • Operating band = 296–383 GHz	Ansys HFSS full wave EM simulator
[36]	Turnstile antenna	1 THz	• Circular polarization • Frequency tunable • Compact • Satcom	• Gain = 0.5 dBi • 30% 3-dB axial ratio bandwidth • 69.79% efficiency	CST Microwave Studio and MATLAB
[37]	Vivaldi patch antenna	0.06125–0.06215 THz	• Metallic on Rogers RT5880 Substrate • PCB technology	• Bandwidth = 80 GHz, • Return loss − 58.83 dB • VSWR = 1.002 • Peak gain − 11.77 dB • Radiation efficiency = 97.40% • Directivity = 11.89 dBi	CST Microwave Studio
[38]	Transmit array	0.12–0.13 THz	• All-dielectric structure • Laser-drilling	• 10 dB wide Bandwidth = 117 to 139 GHz • Gain = 32–34 dB, • Radiation Efficiency = 95%	Ansys HFSS full wave EM simulator
[39]	Patch Antenna and Antenna Array	0.135–0.155 THz	• Megtron 7N substrate • PCB technology	• At 150 GHz, Insertion loss of − 1.9 dB/cm, 1.8 dB/cm for microstrip line and coplanar waveguide respectively • Bandwidth-14% • Gain = 14 dBi	Ansys HFSS full wave EM simulator
[40]	THz Circularly Polarized Lens Antenna	0.24–0.32 THz	• High-temperature resin • 3D Printing	• 1 dB gain bandwidth = 13.3% • 3 dB axial ratio bandwidth = 18.8% • Directivity = 30.8 dBic	Ansys HFSS full wave EM simulator

Table 3 Summary of Fabrication Technology, Advantages, Disadvantages, Applications and Challenges of few previous works

Ref #	Fabrication technology	Advantages	Disadvantages	Applications	Challenges
[37]	PCB technology	• Enhanced Radiation Performance • Strong gain • Directivity	• Fabrication Challenges • Environmental Sensitivity	• Wireless communications • Video-rate imaging • Spectroscopy • Doppler radar • Object Imaging • Smart City Technologies	• Material Limitations • Heat Dissipation • Cross-Talk and Interference
[24]	PCB technology	• Cost-Effective Manufacturing • Common-Mode Current Suppression	• Potential Size Constraints	• Internet of Things (IoT) • Wireless Sensors • Automotive Applications	• Manufacturing Tolerances • Material Limitations
[38]	Laser-drilling	• All-Dielectric Structure • Zero Back-Scattering • Beam forming Capability	• Complexity in Design • Potential Losses in Fabrication	• Wireless Communications • Antenna Beamforming • Imaging Systems	• Cost of Advanced Manufacturing • Integration with Existing Systems
[39]	PCB technology	• Wide-Band Performance • High Gain	• Complex Manufacturing • Potential for Fabrication Variability	• Telecommunications • Phased Array Systems • Radar Systems	• Thermal Management • Cost Management
[40]	3D Printing	• High Gain • Broad Bandwidth • Circular Polarization • Cost-Effective Fabrication • Lightweight Design	• 3-D Printing Constraints • Narrow angle of operation	• Terahertz Communication • Satellite Communication • Aerospace and Defense	• Integration with Feed Sources • Precision Manufacturing
[34]	Wire-cutting EDM	• High Efficiency • Strong Circular Polarization • Accurate Fabrication	• Material Constraints • Complex Fabrication Process	• Wireless Sensing and Monitoring • High-Data-Rate transmission • Aerospace and Defense	• Testing Limitations • Integration Issues

Table 4 Summary of Various Implementation Methods and Technologies of few recent 6G wireless communication network

Ref #	Technology/implementation method	Algorithms/adapted techniques	Advantages	Limitations	Description
[46]	Reconfigurable Intelligent Surfaces	Blind beamforming	• Reduced Computational Cost, • Statistical Approach, • SNR boost of up to 17 dB at 2.6 GHz	• Dependency on Statistical Measurements • Random Phase Shifts • Complexity in Implementation	Enhancement of Multi-IRS Performance with Blind Beamforming without Channel Estimation
[47]	Mobile and cell-free user-centric networking	multiple-carrier division duplex scheme	• Wired Fronthaul Elimination • Efficient Use of THz Bandwidth • Dynamic AP Clustering • Reducing infrastructure costs	• Sensitivity to Channel Conditions • Implementation Complexity	End-to-end performance improvement using a duplex frame structure utilizing multiple carrier division
[48]	Terahertz Sensing and communications	Ray-tracing-statistical hybrid model	• High Bandwidth Utilization • Temporal and Spatial Consistency Verification • Modeling of Path Loss • Hybrid Model Proposal	• Impact of Antenna Configuration, • Scalability Issues	Measurements of the channels at 201–209 GHz in indoor communication environments
[49]	Ultra massive MIMO	Three dimensional 6G-non stationary geometry based stochastic model	• Exploration of Unique Channel Characteristics • Development of a Generalized Model • Identification of Channel Hardening effect	• Sparse Property Findings • Challenges with Non-Stationarity	Ultra massive MIMO communication systems at the 5.3 GHz band are investigated using a statistical model that looks at several antenna array topologies
[50]	AI (artificial intelligence)	Multi-agent reinforcement learning	• Adaptability to Complex Tasks • Autonomous Decision-Making • Research Opportunities	• Performance in Uncontrolled Environments • Potential Overfitting	Multi agent reinforcement learning is utilized in the emergent communication network to integrate autonomous decision making skills

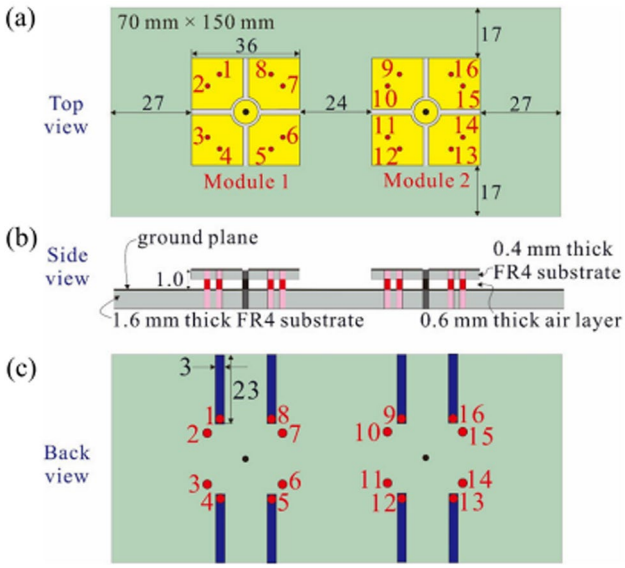

Fig. 2 Geometry of the 1 × 2 module array with two 8PM antenna modules mounted on a ground plane. **a** Top **b** Side view **c** Back view [11]

2 Mid-frequency 6G antenna architectures

Table 1. Presents a summary of the key characteristics of mid-frequency 6G antennas as documented in recent publications.

2.1 8-Port MIMO antenna module

The antenna discussed in [11] operates within the 6 GHz frequency bands, and it has been shown that using MIMO with eight spatial streams, it can attain a spectral efficiency exceeding 56 bps/Hz. Figure 2 shows the geometry of the 1 × 2 module array with two eight-port multiple-input and multiple-output (8PM) antenna modules mounted on a ground plane. (a) Top (b) side view (c) Back view. This antenna is an 8PM antenna module designed to provide eight uncorrelated waves operating in the 6.425–7.125 GHz range using four patch antennas. These patch antennas feature dual polarization, and the entire module is designed to be compact, with each antenna element taking up just 0.074λ2 of area. The antenna has been extended to a 1-by-2 8PM configuration and tested to provide up to 10 Gbps data throughput with 200 MHz bandwidth, thereby enabling a spectral efficiency (ηs) exceeding 56 bps/Hz. This achieved ηs is thrice than that of a 4-by-4 MIMO for 5G operation at 3.5 GHz. The ports 1–8 of the 8PM antennas are excited to generate eight uncorrelated waves at the desired frequency bands. Port isolation is achieved by adding a shorted disk in the four dual-polarized antennas, which slightly diverts the surface currents. This antenna has been applied to a 16-by-8 MIMO test bed system and measured for its bit error rate, throughput, spectral efficiency, and Signal-to-Noise ratio (SNR). The results obtained from these measurements are summarized in [11].

2.2 4-port MIMO antenna module

6G devices are anticipated to support more MIMO spatial streams than their 5G counterparts. As a result, this antenna is targeted to operate in 7.025–8.4 GHz to achieve larger spectral efficiency. Figure 3 shows geometry of the low-profile four-port MIMO (4PM) antenna module. (a) Top and side views. (b) Perspective view. The antenna [12] is constructed using 4PM antenna modules that forms 16-port closely spaced 2-by-2 module array. Since 16-port structures occupies large device real estate, using 4-port MIMO antenna modules makes the antenna low profile to support eight spatial streams with the ηs of 56 bps/Hz. Simulation of this structure reveals that the antenna resonates at approximately 7.3 and 8.3 GHz with a 3:1 VSWR, a common standard for mobile antennas. These results are attributed to the antenna structure: four square top sub patches with truncated inner corners are printed on a FR4 substrate, separated by a layer of air.

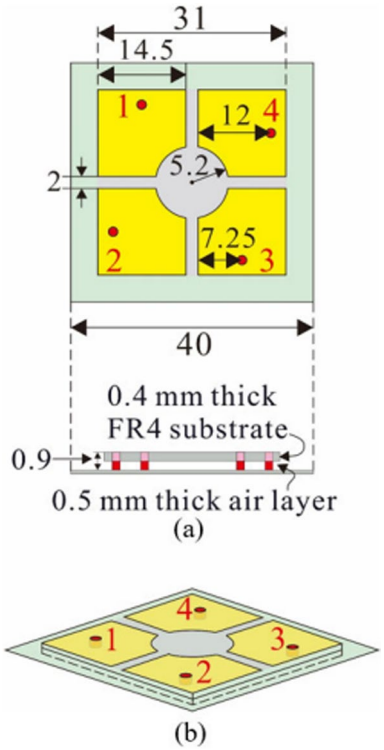

Fig. 3 Geometry of the low-profile four-port MIMO (4PM) antenna module. **a** Top and side views. **b** Perspective view [12]

2.3 Planar lens antenna for X-band 6G applications

High-gain antennas are in demand when it comes to compensate free space path loss in higher operating frequencies. This is applicable in sensing and massive MIMO systems [13, 14]. Massive MIMO systems can employ EM lens with large antenna array to tap into benefits of energy focussing and spatial interference rejection [15, 16]. The Lens antenna array focus signals into distinct paths i.e. focus energy based on Angle of Arrival (AoA) of signals reducing the need for multiple RF chains [17, 18].

The contour map of the power of the signals received by various lens array elements for signals coming at (θ, φ) = (0,0) and (0, −15°), respectively, is displayed in Figure 4. The experimental verification confirms that the energy focusing antennas of lens arrays fluctuate with the orientations of the signals when a signal arrives at a different direction (θ, φ) = (0, −15°). These antennas are relocated to those with indices around (3, 4).

In [19], a novel design is suggested to enhance antenna gain through a single-layer metasurface comprising several circular metal patches combined with rectangular slots. These slots determine polarization of antenna. This paper also compares non-resonant and resonant planar lens antenna designs. The non-resonant planar lens antennas require high permittivity materials which makes fabrication unfeasible. But using metasurfaces, one can design a high gain planar antennas without high permittivity materials. The shape of the planar lens is optimized to achieve an increased gain for a single patch antenna, which rises from 7.2 dBi to 16 dBi at 10 GHz and reaches 12.8 dBi at 10.4 GHz within the X-band spectrum. This eliminates the necessity for an array feeding network, thereby reducing losses generated by feed. These factors contributed to high gain planar structures.

2.4 Glass shaped patch antenna for UWB and 6G applications

To provide reliable 6G networks in urban areas, higher data capacity is required, and the frequency of interest that can achieve this desired outcome is centimetric waves. The centimetric wave bands are also referred as mid-band 6G spectrum that pans from 7–20 GHz will be one of the promising frequency bands that can provide a robust coverage in urban areas. The ideal antenna candidate to meet these requirements are patch antennas because they are easy

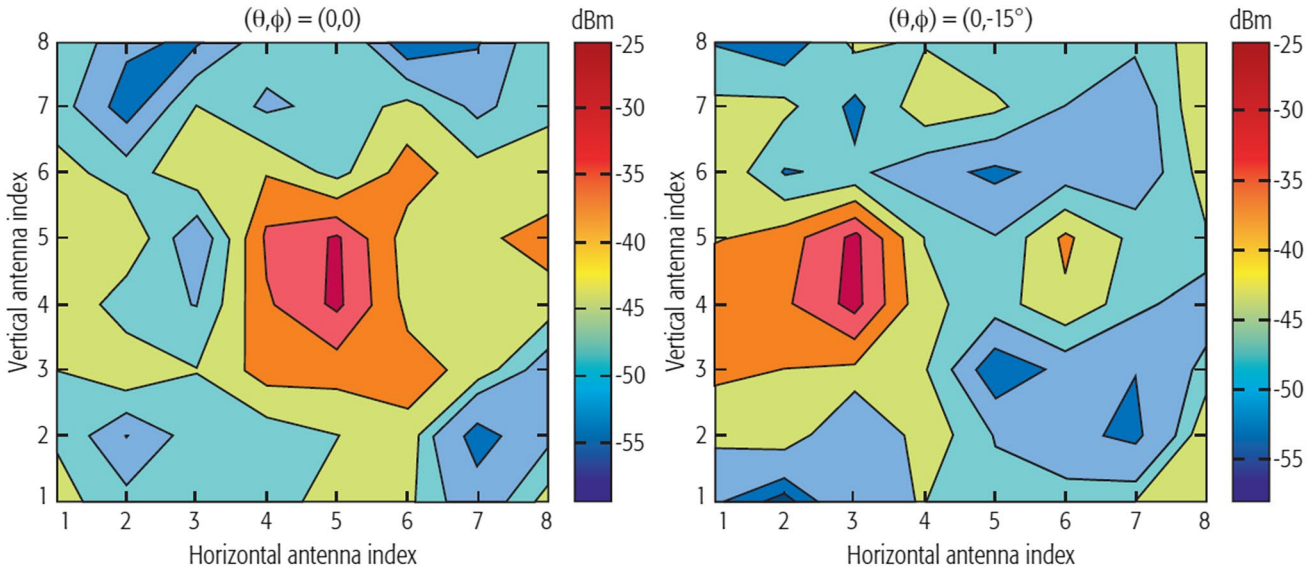

Fig. 4 Contour plot of the received signal power by different elements of the lens array [17]

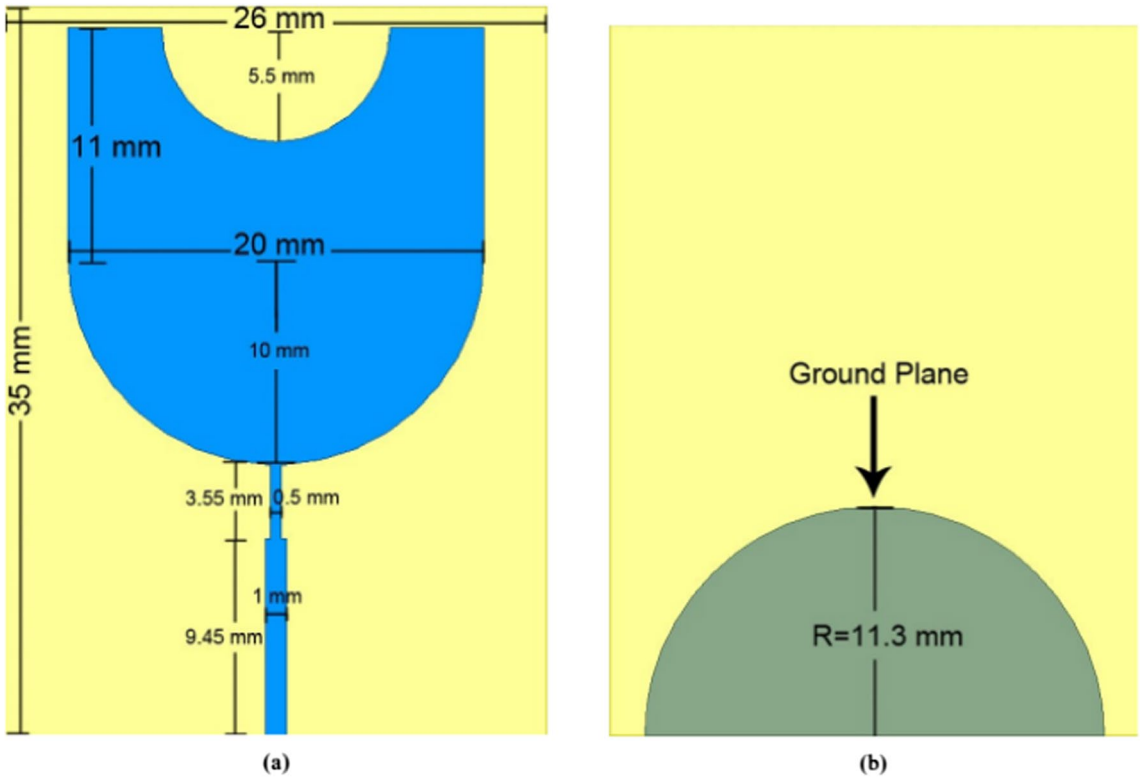

Fig. 5 **a** Top view and**b** bottom view of the glass shaped antenna [20]

to integrate in a PCB [20]. The patch in [20] is form of a glass to enhance the bandwidth. Figure 5 shows (a) Top view and (b) bottom view of the glass shaped antenna.This structure is fed through a microstrip quarter wave transformer for impedance matching purposes. The ground plane is also etched with a semi-circular is etched to further enhance the impedance bandwidth. This configuration provides an UWB antenna that operates between 2.69–20.05 GHz with a fractional bandwidth of 152.68% and a VSWR < 2 for the entire operating frequency band.

2.5 Slotted stacked patch antenna array for 6G satellite mobile communication systems

Another antenna candidate discussed in [21] is used to increase the data capacity is active antenna array. The frequency of interest that was chosen is in K/Ka band and this antenna array is targeted to provide beam steering patterns for 6G TX/RX satellite mobile communication systems. Figure 6 shows the 3D view of the square-ring patch 8 × 8 sub-antenna. The first step in designing this antenna is to calculate the link budget of a satellite link and determine its gain. The antenna gain has been found to be a minimum of 35 dB. The next step in the active antenna design process is choosing an ideal candidate for antenna element that meet the requirements. The filtering antennas or filtennas are chosen because they do not require additional filtering systems. For an element in the antenna array, a patch antenna that resembles like a stacked square-ring is selected for its filtering capability, simple design, and low cost. The stacked square antenna consists of two square rings that are stacked on each other to increase the operating bandwidth and decrease the Z_{in}. The radiation pattern is notably wide, exhibiting a peak directivity perpendicular to the antenna's plane and null directions parallel to the ground plane. This element is extended to an 8-by-8 array comprising of 64 elements and this array resonates at 19.5 GHz and 29.5 GHz with the directivity of 23.3 dBi at 30° scanning. The paper discusses that if 8-by-8 array is extended to 64-by-64 antenna array, then the directivity and gain can be improved.

2.6 Sandwiched PRS Fabry–Perot antenna

Since 6G RF architecture demands a compact PCB real estate, the choice Fabry–Perot (FP) antennas come to mind. FP antennas are favored in wireless communications for their high gain characteristics, though this high gain comes at a cost of larger cavity height. Figure 7 shows the (a) Side view of the FP antenna, (b) geometry of the slit radiator. The FP antenna architecture incudes a substrate, Partially Reflective Surfaces (PRS), and one or more superstrates.The distance between substrate and superstrate, cavity height, is expected to be λ/2 for optimal Aperture Efficiency (AE). But with demand of compact RF architecture, the antenna in [22] proposes a novel idea in reducing the cavity height up to λ/17 without compromising AE. The lower cavity height is achieved by sandwiching PRS between two superstrates. This aided in reducing the cavity height. The prototype antenna resonates at 25.3 GHz with AE of 79.4% and a gain of 12.35 dBi. Due to these simulated results, it makes a promising 6G antenna candidate.

2.7 Wearable ring metal-dielectric and DR antennas

The demand of light-weight antennas in 6G communications motivated to design antennas that are light-weight and economical to fabricate. Figure 8 shows the Patch antenna integrated into a wearable ring (a) top view, (b) side view .To do this, the paper [23] introduces Fused Filament Fabrication (FFF) to fabricate antennas. FFF uses an in-house machine to fabricate metal-dielectric antennas thus 3-D printing of metal and the substrate layer. This paper uses FFF to fabricate patch antenna that can be integrated to a wearable ring and a Dielectric Resonator Antenna (DRA). The advantages of using this fabrication methodology are to keep the fabrication cost down. The fabricated patch antenna was measured in free space using a hand phantom. This antenna resonated around 28 GHz with 0.6 GHz of impedance bandwidth. This

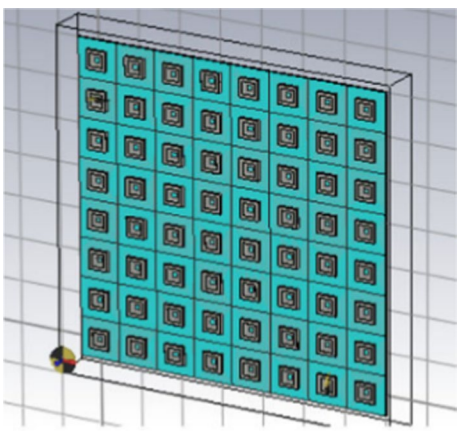

Fig. 6 A 3D view of the square-ring patch 8 × 8 sub-antenna [21]

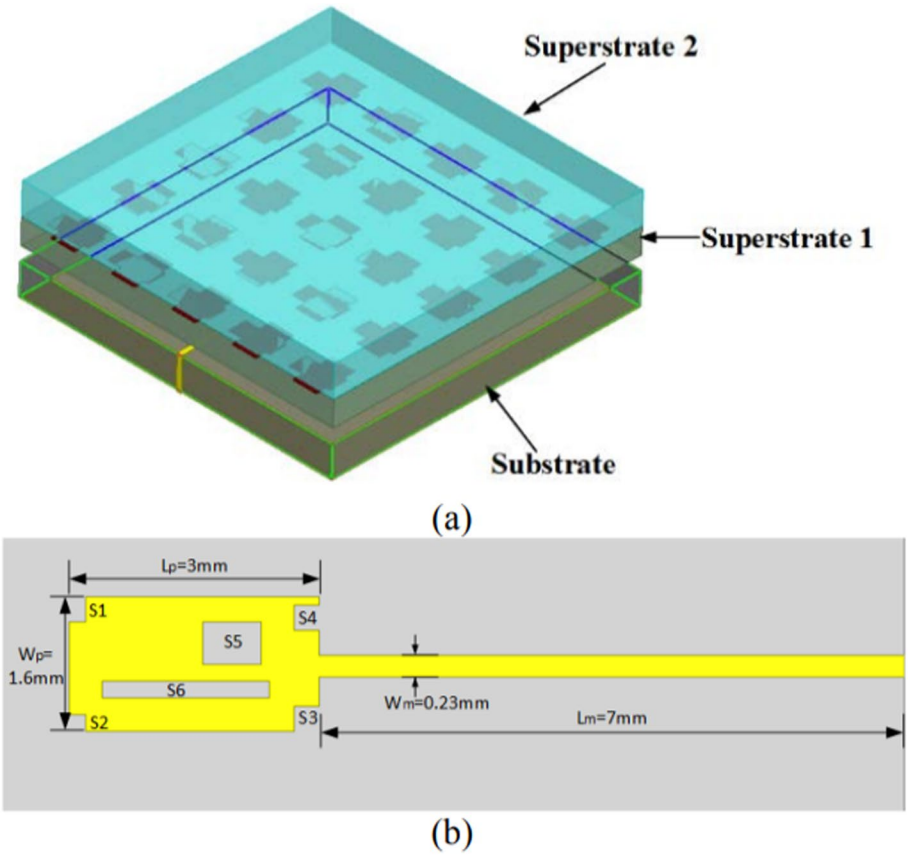

Fig. 7 **a** Side view of the proposed structure **b** geometry of the slit radiator [22]

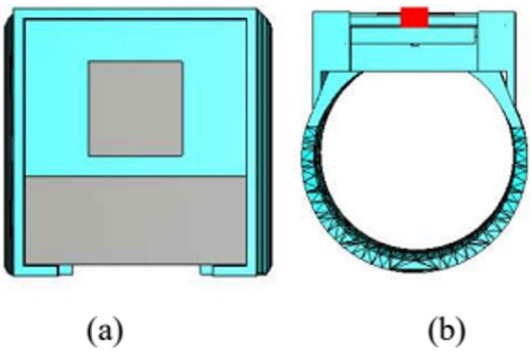

Fig. 8 Patch antenna integrated into a wearable ring: **a** top view **b** side view [23]

paper also discusses about fabrication of DRA to emphasis the future scope of fabricating future 6G antennas. The DRA resonates at 13.5 GHz and 0.5 GHz impedance bandwidth with the radiation gain above 6 GHz.

2.8 Wideband Antenna-in-Package

The Antenna-in-Package (AiP) is commonly used in 60 GHz and above applications. The AiP are cost effective and make the antennas compact. This also means that antenna and RF systems share very small physical distance in PCBs, and this produces EM interference. The EM interference is introduced by common mode currents and common mode suppression techniques in PCBs are very hard to achieve due to small coupling distance, high permittivity of the material, etc., To overcome the challenges, a low-cost antenna AiP antenna is designed in [24] with wideband common-mode chocking characteristics. Figure 9 shows the evolution of the proposed antenna. (a) Wideband, High-Efficiency Electromagnetic Structure (WHEMS) with a back plate and metal backing cavity. (b) Ideal model of the proposed antenna. (c) AiP implementation of the proposed antenna in PCB technology. The antenna is a WHEMS featuring a backing cavity. Within this cavity, an enhanced quarter wave transformer, known as a radiating choke, is embedded. This choke effectively

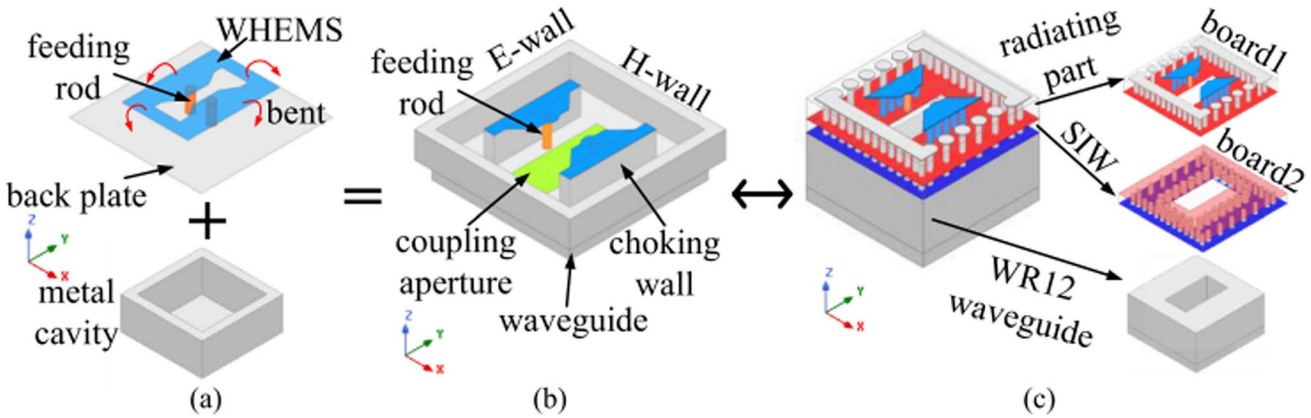

Fig. 9 Evolution of the proposed antenna. **a** WHEMS with a back plate and metal backing cavity. **b** Ideal model of the proposed antenna. **c** AiP implementation of the proposed antenna in PCB technology [24]

suppresses both common-mode and radiation currents. The structure demonstrates a 22% impedance bandwidth ranging from 60-75 GHz, with a gain of 8–10 dBi.

2.9 mm-wave conical-beam antenna

Another compact antenna is discussed in [25] which is targeted for mm-wave low-earth orbit (LEO) systems. Figure 10 shows the Proposed ME CB antenna.This antenna is a conical-beam (CB) antenna that operates in E-band (71–86 GHz). Compared to the existing CB antennas this antenna has a high gain of 12.05 dBi at 76 GHz and wideband planar antenna with an impedance bandwidth of 40.9% (59.38–89.95 GHz). The high-gain and wideband characteristics of this antenna is achieved by the probe excitation of electric and magnetic dipoles. The realization of these electric dipoles takes the shape of two annular rings divided into eight annular sectors. And the magnetic dipoles are realized by five vias that are drilled into each annular sector. But this single layer structure has a constraint on the feeding design and imposed a limit on the number of elements. This resulted in poor conical radiation. To generate a good conical radiation a multi-stage circular-cavity substrate integrated waveguide structure is designed and that helped to control the TM_{010}/TM_{020} resonant modes.

2.10 Tooth-shaped antenna

The 76–81 GHz frequency band is used for Autonomous Vehicle Applications (AVA) and the RADAR (Radio Detection and Ranging) systems that are designed to aid the AVA applications to understand the surrounding environments. To do this, these applications require high gain antennas with a broad field view and a narrow beam in azimuth and elevation direction. Figure 11 shows the Tooth-shaped patch antenna. The paper [26] compares a conventional insert-fed patch antenna and how its performance can be improved by using eight equally spaced tooth-shaped slots and two slots at the lower edge of the antenna. Because of its true input admittance, the tooth-shaped antenna design makes it ideal for use in both Long-Range Radar (LRR) and Short-Range Radar (SRR) applications. It resonates at 77 GHz, offering a gain

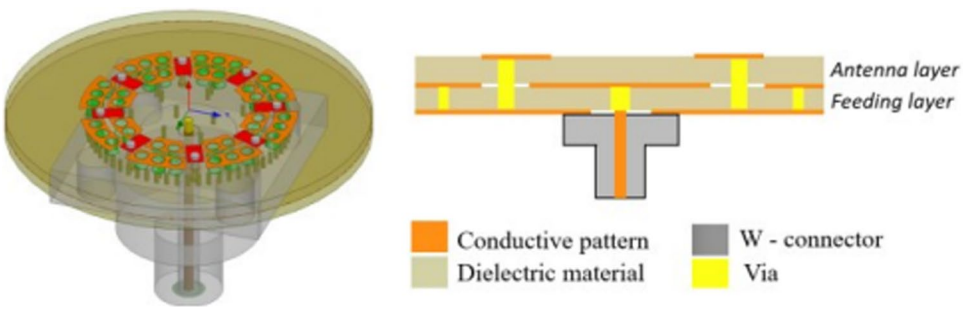

Fig. 10 Proposed ME CB antenna [25]

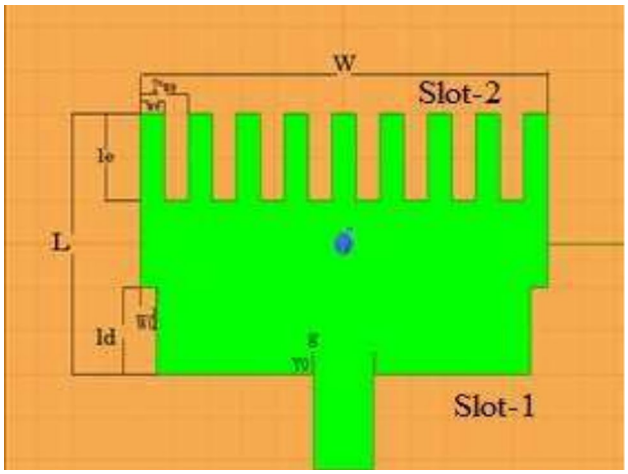

Fig. 11 Tooth-shaped patch antenna [26]

of 9.4 dB and a current distribution of 1.36 × 103 A/m. At this resonant frequency, the antenna's return loss is simulated at – 37.9441 dB.

3 High-frequency band 6G antennas

Table 2 presents a summary of the key characteristics of high frequency 6G antennas as documented in recent publications.

3.1 110 GHz antenna array module using AiP

Sub-Terahertz (Sub-THz) frequencies are one of the promising frequency bands in 6G communications. This is primary because we can optimize our systems for high data rate. Due to the small wavelength in Sub-THz frequencies, AiPs are best suited to realize antenna array module. In this paper [27], a 110 GHz antenna array module was realized in AiP. At Sub-THz, AiP radiation performance will vary because most System-in-Package (SiP) fabrication processes have been designed for packaging low frequency RF systems. Conventional SIP architectures employs even substrates in total: A core substrate with thicker thickness for mechanical support and this core substrate is stacked with three thinner substrates top and bottom of the core substrate with prepreg materials. Figure 12 shows the Stacked dielectric substrates to design the Sub-THz AiP. In this paper, two AiP architectures are discussed: In this first architecture, a thicker core is used. The thickness of the first AiP with all the layers is 850 µm. This includes ground and metal planes with metal via-pad and anti-pad. For the second architecture, a thinner core is used, and it brings down the thickness to 400 µm. In the metal layer, a rectangular metal patch radiator is placed. While simulating it is observed that the AiP with the thinner thickness produce larger bandwidth of 6.6 GHz at 110 GHz resonant frequency. When the antenna is extended to 2-by-2, 4-by-2,

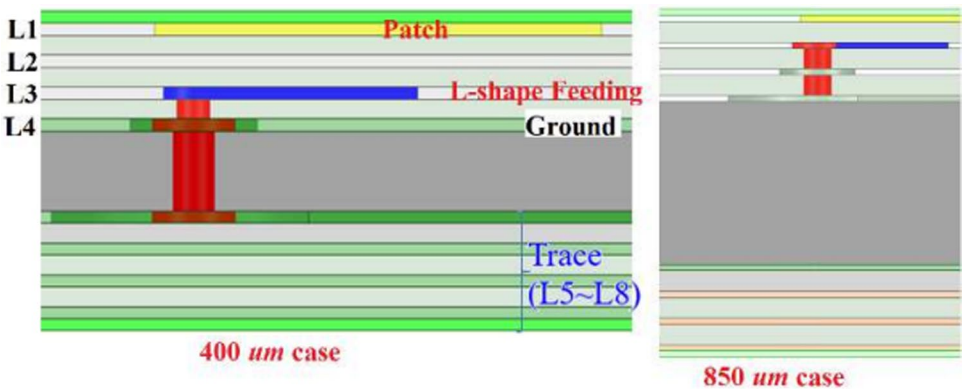

Fig. 12 Stacked dielectric substrates to design the Sub-THz AiP [27]

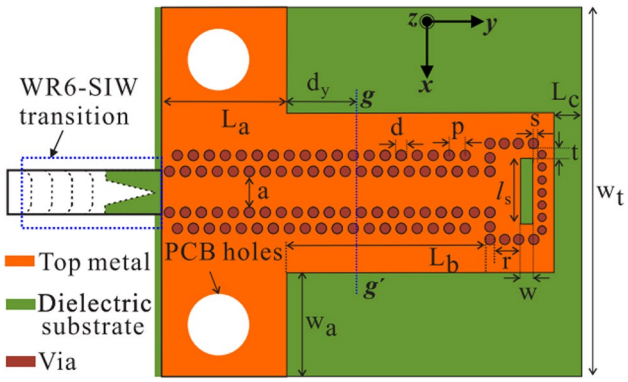

Fig. 13 Antenna with WR6-SIW transition [28]

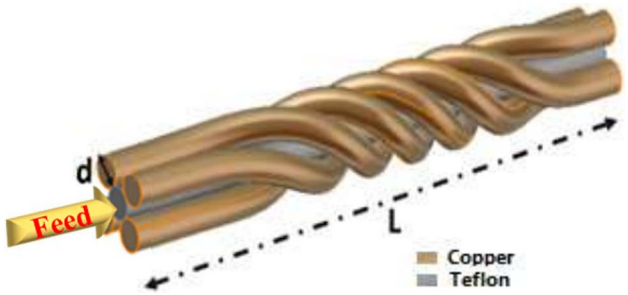

Fig. 14 Leaky Wave Antenna [29]

4-by-4, 4-by-4, 8-by-4, and 8-by-8, it is observed that the bandwidth and gain increased. For 8-by-8, the AiP exhibits a 19.65 dBi gain and 9.19 GHz bandwidth.

3.2 Substrate integrated waveguide (SIW) based slot antenna

This paper [28] also proposes a D-band (110–170 GHz) antenna that aims to provide higher data rates. The antenna is chosen to be a wideband PCB based SIW slot antenna designed. To support higher order modes, a wide cavity is selected. Figure 13 shows the Proposed antenna with WR6-SIW transition. The antenna architecture comprises of top and bottom metal layers, and they are joined to create SIW line and cavity. The two layers communicates with arrays of vias, and their dimensions are optimized to ensure that the radiation loss is less than or equal to – 0.06 dB throughout the D-band. The top metal layer is etched with a rectangular slot to support the antenna performance. Upon simulation, the antenna resonates at six different frequencies in the D-band. The modes supported by this structure are TE_{310} at 114.2 GHz and TE_{210} at 134.75 GHz. The other four resonance frequencies, identified at 124 GHz, 144 GHz, 154 GHz, and 160 GHz, result from hybrid modes. The first two are created by the merging of TE_{310}–TE_{120} and TE_{120}–TE_{220} modes, respectively, while the last two originate from the combination of TE_{220}–TE_{320} modes.

3.3 Leaky wave wire antenna

The antenna in [29] is a leaky wave wire antenna which is also another D-band antenna that operates at 120 GHz with a simulated gain of 9.9 dBi. Figure 14 shows the Leaky Wave Antenna. The design of the antenna features four metal wires wrapped around a Teflon rod, with each wire being twisted at a rate of 520°. This antenna architecture is simple and does not require tedious fabrication process. However, this paper does not cover feeding mechanisms for exciting this antenna, as designing and selecting optimal feeding mechanisms for these architectures poses significant challenges. If properly excited, this architecture can be used for 6G communications.

3.4 Stacked patch 4-by-4 antenna array

The antenna in [30] is a stacked patch 4-by-4 antenna array that was built to target data-intensive 6G applications including driver-less vehicles, extended reality, and broadband plus. To support 100 GB/s application, the antenna must support at least of 25 GHz bandwidth. Figure 15 shows the D-band stacked patch antenna design. (a) PCB stack-up (CORE:

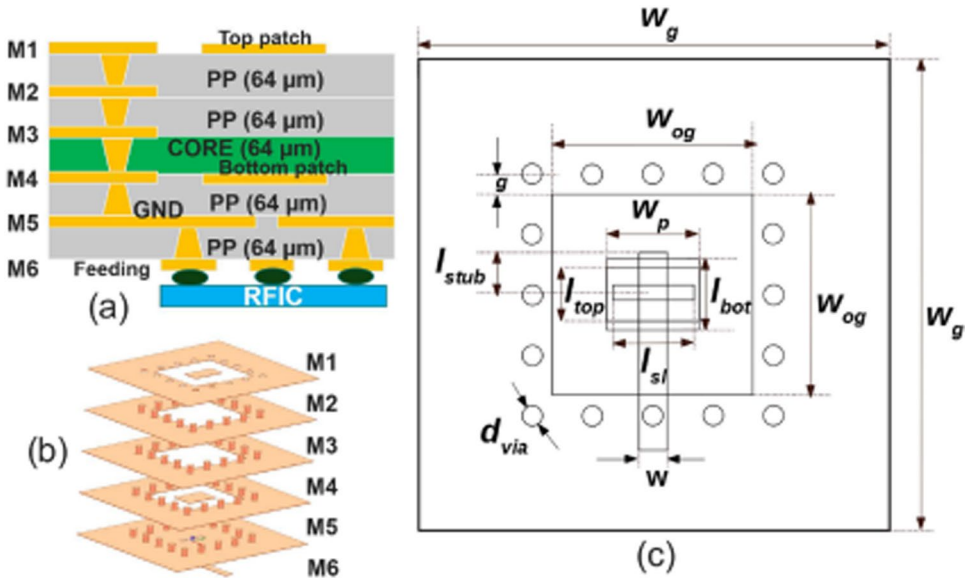

Fig.15 D-band stacked patch antenna design. **a** PCB stack-up (CORE: core substrate. PP: prepreg). **b** Exploded view. **c** Top view and physical parameters of antenna structure [30]

core substrate. PP: prepreg). (b) Exploded view. (c) Top view and physical parameters of antenna structure. The proposed design consists of six conductor layers. In these six layers, the ground plane, microstrip feeding network, top and bottom patches can be found. Two ground layers with no connection are placed between the top and bottom patches to construct via barriers. Surface waves between each antenna element are suppressed as a result. Upon simulating a single antenna element, the structure yielded the 40 GHz bandwidth and 6.9 dBi gain. This structure is extended to 4-by-4 planar array and measured to find the resonance is at 140 GHz featuring a 35 GHz bandwidth that spans from 123–158 GHz, along with a gain of 17.5 dBi.

3.5 MIMO D-band antenna array

The antenna described in [31] is another promising candidate for 6G communication. Figure 16 shows the geometry of the low profile antenna (a) top view (b) metric view. The antenna consists of 8-by-8 antenna arrays that provides a

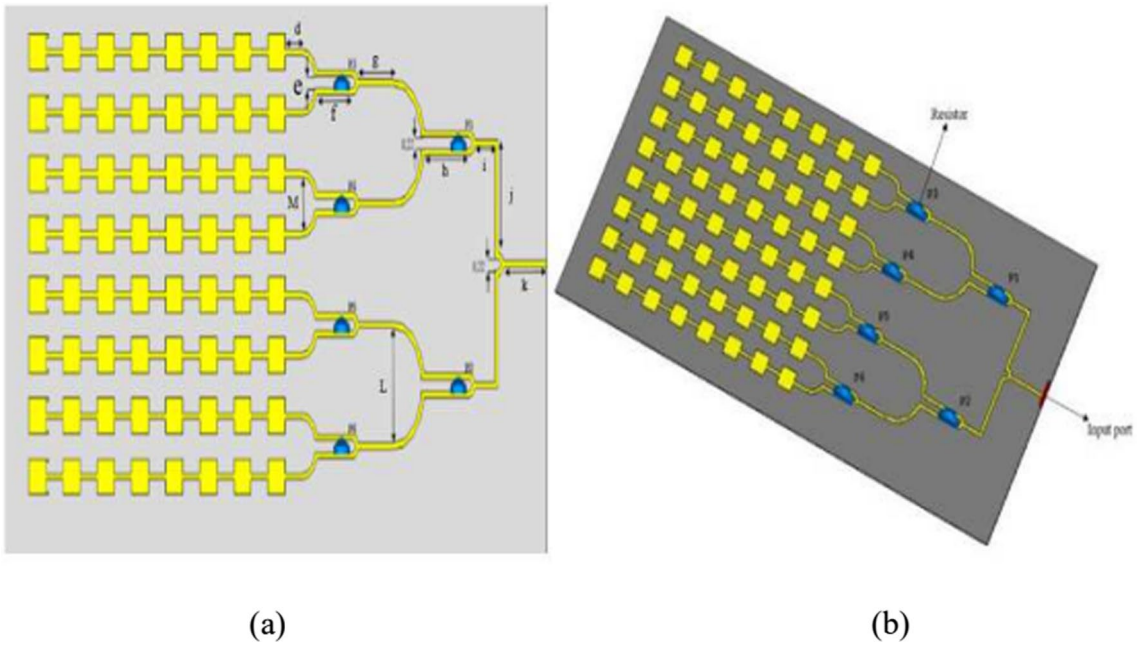

Fig. 16 Geometry of the low profile antenna **a** top view **b** metric view [31]

gain of 18.3 dB and a bandwidth of 17 GHz from 142-155.5 GHz with 150 GHz being resonant frequency. The design process involves first constructing 1-by-8 MIMO patch array and each element of this patch array is cascaded using series feed. After constructing 1-by-8 array, an 8-by-8 array is formed with 8 elements of 1-by-8 array. The 8-by-8 array is connected using a 50 Ω 1-to-8 Wilkinson power divider. By connecting the antenna in this configuration, the antenna provided a wider bandwidth which will allow this antenna to transmit signals at higher data rates.

3.6 Symmetrical multi slot THz microstrip antenna

The antenna described in [32] features a silicon substrate with a butterfly-shaped radiation arm that is symmetrical from left to right, and it utilizes a lumped port for excitation. Figure 17 shows the Antenna 3 and specific structure of "loop" patch. The antenna is constructed in multiple iterations to improve the performance and support 6G communication requirements. In the first iteration, the antenna resembles a traditional bow tie with slots. In addition to this, a circular and semi-circular patch was etched at the symmetry and two ends of the radiation arms, respectively. The antenna upon simulation reveals that it resonates at 228 GHz and 243 GHz with the 31.4 GHz operating bandwidth and 7.44 dB gain. To further improve the performance, in the second iteration, a vertical rectangular slot is cut into the center of the structure. This improved the current distribution, operating bandwidth, and gain. In the third iteration, a circular groove was added to the left and right of the central symmetry of the antenna. This moved the resonant frequency to 217 GHz and 228 GHz with gain of 3.7 dB and 4.5 dB, relatively. The inclusion of a circular groove expanded the operating bandwidth to 33 GHz, resulting in a relative bandwidth for the structure of 41.25%.

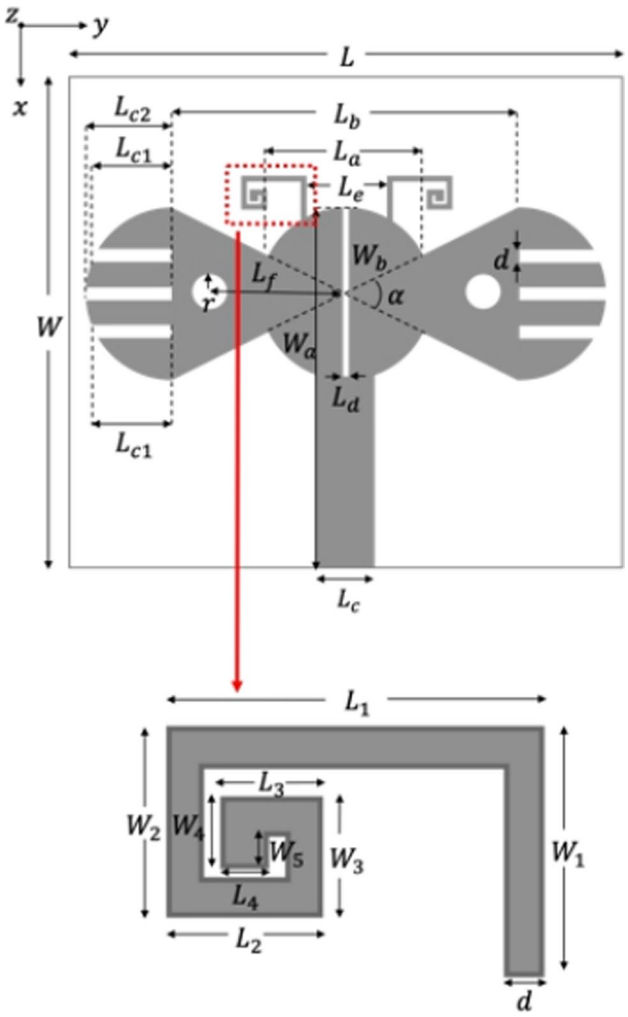

Fig. 17 Antenna 3 and specific structure of "loop" patch [32]

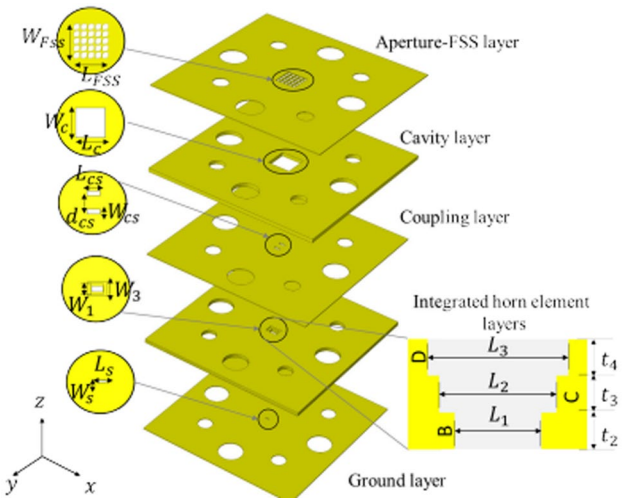

Fig. 18 Exploded view of the antenna [33]

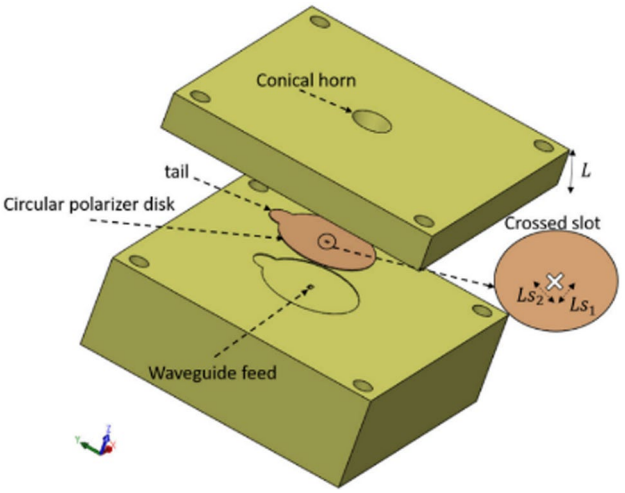

Fig. 19 A 3-D exploded view of the antenna [34]

3.7 Circularly polarized Sub-THz four-layer antenna

The antenna designed in [33] operates in sub-THz frequency region to combat high atmospheric attenuation, and to support high data rates and large bandwidths. However, in sub-THz band, using a relatively thick substrate produces surface waves and this in turn will result in narrower bandwidth antennas. To avoid this issue, the antenna is designed using brass and it is Circularly Polarized (CP). Figure 18 shows the Exploded view of the antenna.The antenna consists of four layers: radiating window, an excitation layer, an air cavity, and a coupling layer. The radiation characteristics is like of an Air-filled Channelized Coplanar Waveguide (ACCPW) and a 300 GHz WR-3 waveguide is used to center feed the structure. The antenna offers a 12 GHz axial ratio bandwidth from 278.2–290.2 GHz, within an 8.9% impedance bandwidth from 270-295 GHz and boasts a gain of 11.9 dBic and 95.1% efficiency. Its compact size of 2.25λ -by- 2.25λ -by- 0.5λ at 285 GHz makes it ideal for next generation sub-THz 6G applications.

3.8 Circularly polarized horn antenna

Another CP antenna for 6G applications were discussed in [34], but this is a horn antenna. Figure 19 shows the 3-D exploded view of the antenna.This horn antenna is fabricated using the wire Electrical Discharge Machining (EDM) method. Designed for operation at 300 GHz, the antenna features a WR-03 rectangular waveguide feed, a circular polarizer disk, and a conical horn. The circular polarizer is made up of crossed slots of unequal lengths, which are

perpendicular to each other. Adjusting the lengths of these slots allows for the observation of the Circular Polarization (CP) radiation pattern. The antenna provides a 20% impedance bandwidth, ranging from 270 GHz to 330 GHz, with a reflection coefficient of ≤ − 15 dB. Additionally, it offers a 7 GHz axial ratio bandwidth between 309-316 GHz, achieving a minimum axial ratio of 1.15 dB at 312 GHz.

3.9 THz dipole reflector antenna

6G wireless communication is expected to operate in THz to provide higher data rate compared to 5G and other older communication standards [4]. One of the promising antenna candidate is proposed in [35]. The antenna is simple dipole with reflectors and directors that operates between 295–400 GHz with 33.8% impedance bandwidth. Figure 20 shows the Top view of the single element with a reflector .The antenna resonates at 310 GHz and uses indium phosphide and benzo-cyclo-butene as substrates. Gold is used to construct dipole, reflector, and half-circle shaped directors. The overall gain through simulation is observed to be 7.27 dBi. Although the proposed antenna features a simple design, the selection of materials for its substrates and conducting layer renders it both costly and specialized.

3.10 6G Turnstile antenna

The study [36] explores a 1 THz graphene-based turnstile or crossed-dipole patch antenna, chosen for graphene's superior properties over copper in conductivity, tensile strength, and current density at THz frequencies, making it ideal for THz 6G antennas. Graphene also enables Transverse Magnetic Surface Plasmon Polariton (TM SPP) waves. Figure 21 shows the Graphene THz Turnstile Antenna. Constructed from two graphene dipoles on an epoxy and silica substrate, electromagnetic simulations show the antenna supports circular polarization with a 30% 3 dB axial ratio bandwidth, 0.454 dBi gain, and 69.79% efficiency. However, its low gain raises questions about its effectiveness for 6G communication.

4 Future direction

Future trends in 6G antenna designs are focused on meeting the demands of ultra-fast data rates, low-latency communication, and enhanced energy efficiency [41, 42]. Here are some key trends:

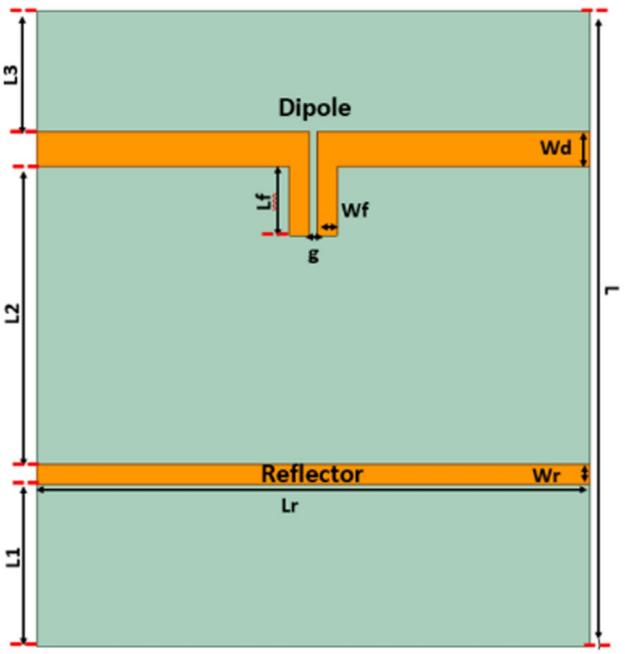

Fig. 20 Top view of the single element with a reflector [35]

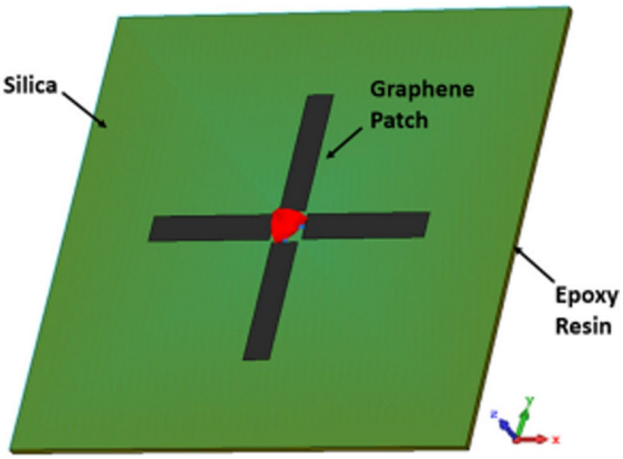

Fig. 21 Graphene THz Turnstile Antenna [36]

4.1 Terahertz (THz) antenna design

Massive bandwidth is available at THz frequencies, which are operated over 100 GHz using 6G antennas [43]. These extremely high frequencies will require antenna designs to be capable of handling smaller, high-gain antennas that can overcome the propagation issues associated with THz signals. Research is being done on materials like graphene and metamaterials to enable a small and effective THz antenna.

4.2 Reconfigurable intelligent surfaces (RIS)

RIS is a method used to modify radio waves without the need of sophisticated signal processing algorithms or active power amplifiers [44]. Real-time wireless signal reflection and refraction on passive, tunable surfaces will be possible thanks to RIS technology. Because RIS-based antenna designs eliminate the need for high-power transmitters, 6G networks will use less energy and be more environmentally friendly.

4.3 Beamforming and beam steering enhancements

6G antenna systems will use AI and machine learning to automatically adjust beamforming. As a result, antennas will be able to automatically modify beam direction and power levels in response to network conditions, user location, and mobility patterns.

In order to reduce interference and improve the signal-to-noise ratio (SNR) for more dependable communication, antenna arrays use beamforming to focus signals into particular places. While digital beamforming uses digital signal processing (DSP) to alter amplitude and phase, analog beamforming uses phase shifters to modify the phase of each antenna element. Performance and complexity can be balanced by combining the two approaches[45].In millimeter-wavelength communications, huge antenna arrays are typically installed at the transmitter and/or receiver to produce massive beamforming gains in order to offset the significant route loss. For millimeter-wave communications, EM-lens enabled MIMO can be used to significantly enhance beamforming performance while lowering hardware and signal processing expenses [17].

4.4 Miniaturization and integration

Future antennas may incorporate flexible, conformal designs for better integration with devices like smartphones, wearables, and even clothing, offering greater flexibility in product design while maintaining high performance.

In summary, 6G antenna designs will focus on ultra-high frequency operation, intelligent beamforming, and integration with smart surfaces, all while enhancing energy efficiency and supporting next-generation wireless applications.

5 Conclusion

In conclusion, this review has detailed around 50 different 6G antenna architectures, spanning mid- (1–100 GHz) and high-frequency (above 100 GHz) bands, providing a broad overview of their capabilities and designs. Through antenna overview tables, we've highlighted the key features of each antenna, arranging them by their resonant frequencies for easy comparison. This paper offers a clear snapshot of the current advancements and future prospects in 6G antenna technology, emphasizing the evolving challenges and innovations in the field of 6G wireless communication.

Acknowledgements The authors acknowledge Panimalar Engineering College, Chennai, India for providing excellent support to this review article.

Author contributions Ameelia Roseline A, supervised the overall progress of the research, offering guidance and expertise in refining the study design, addressing methodological challenges and Final Approval. Pranav Mohan Kumar, played a key role in the initial conceptualization of the research, contributing valuable ideas and insights that shaped the study's direction. All authors were primarily responsible for drafting sections of the manuscript and critically reviewed and edited the manuscript, providing constructive feedback and ensuring the coherence and accuracy of the content.

Funding Not applicable.

Data availability No datasets were generated or analysed during the current study.

Declarations

Ethics approval and consent to participate Not applicable.

Competing interests The authors declare no competing interests.

References

1. Dhinesh Kumar M, Suresh C. Shift to 6G: Exploration on trends, vision, requirements, technologies, research, and standardization efforts. Sustain Energy Technol Assess. 2022;54:102666. https://doi.org/10.1016/j.seta.2022.102666.
2. Shafi M, Jha RK, Jain S. 6G: technology evolution in future wireless networks. IEEE Access. 2024;12:57548–73. https://doi.org/10.1109/ACCESS.2024.3385230.
3. Hua TD, Mohammadi M, Ngo HQ, Matthaiou M. Cell-free massive MIMO SWIPT with beyond diagonal reconfigurable intelligent surfaces. arXiv preprint arXiv. 2024. https://doi.org/10.48550/arXiv.2402.00646.
4. Mohammadi M, Tran LN, Mobini Z, Ngo HQ, Matthaiou M. Cell-free massive MIMO and SWIPT: access point operation mode selection and power control. GLOBECOM. 2023. https://doi.org/10.1109/GLOBECOM54140.2023.10437956.
5. Dikmen O. Pilot assignment for cell free massive MIMO systems: a successive interference cancellation approach. Duzce Univ J Sci Technol. 2024;12(3):1739–51. https://doi.org/10.29130/dubited.1448494.
6. Dikmen O. Performance analysis and simulation of IRS-aided wireless networks communication. Symmetry. 2024;16(2):254. https://doi.org/10.3390/sym16020254.
7. Mukherjee T, Pati B, Panigrahi CR, Bebortta S. Performance modeling of composite fading channels: an application to wearable wireless communication systems. Discov Electron. 2024. https://doi.org/10.1007/s44291-024-00020-3.
8. Singh A, Ritika, Jangid A. A fast and effective approach for microstrip filter design using GA and TL—model. Discov Electron. 2024. https://doi.org/10.1007/s44291-024-00007-0.
9. Zhang Y, Ogurtsov S, Vasilev V, Kishk AA, Caratelli D. Advanced dielectric resonator antenna technology for 5G and 6G applications. Sensors. 2024;24(5):1413.
10. MathWorks documentation for RF Blockset, R2024a. https://www.mathworks.com/help/simrf/index.html.
11. Wong KL, Hong SE, Tseng YS, Li WY. Low-profile compact 8-Port MIMO antenna module and Its 1 × 2 Array for 6G 16 × 8 device MIMO application. IEEE Access. 2023;11:137011–24.

12. Wong KL, Hong SE, Li WY. Low-profile four-port MIMO antenna module based 16-port closely-spaced 2 × 2 module array for 6G upper mid-band mobile devices. IEEE Access. 2023;11:110796–808.
13. Shaikh SA, Tonello AM. DoA estimation in EM lens assisted massive antenna system using subsets based antenna selection and high resolution algorithms. Radio Engin. 2018;27(1):159–68. https://doi.org/10.13164/re.2018.0159.
14. Shaikh SA, Tonello AM. Radio source localization in multipath channels using EM lens assisted massive antennas arrays. IEEE Access. 2019;7:9001–12. https://doi.org/10.1109/ACCESS.2019.2891110.
15. Zeng Y, Zhang R, Chen ZN. Electromagnetic lens-focusing antenna enabled massive MIMO: performance improvement and cost reduction. IEEE J Sel Areas Commun. 2014;32(6):1194–206. https://doi.org/10.1109/JSAC.2014.2328151.
16. Shaikh SA. What you should know about next generation 6g mobile technology. Int J Interact Mob Technol. 2022;16(24):191–203. https://doi.org/10.3991/ijim.v16i24.35335.
17. Zeng Y, Zhang R. Cost-effective millimeter-wave communications with lens antenna array. IEEE Wirel Commun. 2017;24(4):81–7. https://doi.org/10.1109/MWC.2017.1600336.
18. Shaikh MA, Shaikh SA, Shaikh FZ. Location based services for remote education and health institutes using sum-difference signal patterns. Int J Interact Mob Technol. 2022;16(22):4–14. https://doi.org/10.3991/ijim.v16i22.35337.
19. Ramzan M, Sen P. (2022) Dual-band gain-boosted planar lens antenna using a single layer metasurface for 6G applications. Joint European conference on networks and communications & 6G summit (EuCNC/6G summit), Grenoble, France.446–450. https://www.barkhausen institut.org/fileadmin/user_upload/Publikationen/2022/6GSummit_MetaAntenna_2022.pdf.
20. Hyasat YM, Faouri YS. (2022) A glass shaped with circular slot patch antenna for UWB applications and potential 6G wireless communications. 4th IEEE middle east and north Africa COMMunications conference (MENACOMM), Amman, Jordan.106–110. https://ieeexplore.ieee.org/document/9998194.
21. Dastkhosh AR, Naseh M, Lin F. (2021) K/Ka Slotted stacked patch antenna and active array antenna design for a 5G/6G satellite mobile communication system. 13th global symposium on millimeter-waves & terahertz (GSMM), Nanjing, China. 1–3. https://ieeexplore.ieee.org/document/9511995.
22. Chandran PBM, Zheng B, An S, Tang H, Li H, Zhang H. (2018). Sandwiched PRS fabry-perot structure for achieving compactness and improved aperture efficiency. IEEE international symposium on antennas and propagation & USNC/URSI national radio science meeting, Boston, MA, US. 2018: 2043–2044. https://ieeexplore.ieee.org/document/8608652
23. S. Li, P. Njogu, B. S. Izquierdo, S. Gao and Z. Chen. 3D Printing Antennas for 5G and Millimeter Wave 6G Applications. IEEE 33rd Annual International Symposium on Personal, Indoor and Mobile Radio Communications (PIMRC), Kyoto, Japan. 2022; p.1–5. https://ieeexplore.ieee.org/document/9978007.
24. L. Chi, Z. Weng, Y. Qi and J. L. Drewniak. A 60 GHz PCB Wideband Antenna-in-Package for 5G/6G Applications. IEEE Antennas and Wireless Propagation Letters.2020; 19 (11): 1968–72. https://ieeexplore.ieee.org/document/9133305.
25. D. A. Pham and S. Lim. Millimeter-Wave Complementary Planar Antenna with Conical Radiation for 6G Applications. IEEE International Symposium on Antennas and Propagation and USNC-URSI Radio Science Meeting (USNC-URSI), Portland, OR, USA. 2023; 1397–1398. https://ieeexplore.ieee.org/document/10238128.
26. Foysal F, Mahmud S, Baki AKM. A novel and high gain antenna design for autonomous vehicles of 6G wireless systems. International conference on green energy, computing and sustainable technology (GECOST), Miri, Malaysia. 2021; 1–5. https://ieeexplore.ieee.org/document/9538702.
27. Wu KH, Chou HT, Lin DB. (2021) Realization of an 110GHz antenna array module by using AiP technologies for potential 6G applications. International symposium on antennas and propagation (ISAP), Taipei, Taiwan. 1–2. https://ieeexplore.ieee.org/document/9614363.
28. Altaf A, Abbas W, Seo M. A wideband SIW-based slot antenna for D-band applications. IEEE Antennas Wirel Propag Lett. 2021;20(10):1868–72.
29. Sohoo AA, Sohu IA, Seman FC, Ishak NS, Khee YS. Leaky-wave wires antenna for future D- Band 6G communication systems. IEEE international symposium on antennas and propagation (ISAP), Kuala Lumpur, Malaysia. 2023. https://ieeexplore.ieee.org/document/10389162.
30. Dao T, Kearns A, Reyes Paredes D, Hueber G. Wideband high-gain stacked patch antenna array on standard PCB for D-band 6G communications. IEEE Antennas Wirel Propag Lett. 2024;23(2):478–82.
31. Hamad HBi, Hrizi H, Ghnimi S, Latrach L, Gharsallah A. (2023) innovative antenna design for advanced 6G technology. 22nd Mediterranean microwave symposium (MMS), Sousse, Tunisia. 1–5. https://ieeexplore.ieee.org/document/10421039.
32. Xu W, Zhang D, Ding, Juan Y, Bian B , Chen CP . (2021) Symmetrical multi slot terahertz 6G communication application band antenna based on butterfly like structure. International conference on microwave and millimeter wave technology (ICMMT), Nanjing, Chinapp. 1–3. https://ieeexplore.ieee.org/document/9618180.
33. Kumar S. Kumar S. (2023) A circularly polarized Sub-THz antenna for 6G wireless communication. IEEE microwaves, antennas, and propagation conference (MAPCON), Ahmedabad, India. 1–5. https://ieeexplore.ieee.org/document/9525377.
34. Aqlan B, Himdi M, Le Coq L, Vettikalladi H. Sub-THz circularly polarized horn antenna using wire electrical discharge machining for 6G wireless communications. IEEE Access. 2020;8:117245–52.
35. Vadlamudi R, Kumar DS. (2023) Design of a THz antenna with broadband radiation characteristics for 6G applications. IEEE wireless antenna and microwave symposium (WAMS), Ahmedabad, India. 1–4. https://ieeexplore.ieee.org/document/10242972.
36. Sharma A, Vishwakarma KD. (2022) Graphene based turnstile antenna for terahertz (6G) applications. URSI regional conference on radio science (URSI-RCRS 2022, IIT Indore. 1–5. https://www.ursi.org/proceedings/2022/RCRS2022/papers/SPCSharmaAmit.pdf.
37. Kushwaha RK, Karuppanan P. Design and analysis of Vivaldi antenna with enhanced radiation characteristics for mm-wave and THz applications. Opt Quant Electron. 2019;51(9):309. https://doi.org/10.1007/s11082-019-2032-4.
38. Emara MK, Stuhec-Leonard SK, Tomura T, Hirokawa J, Gupta S. Laser-drilled all-dielectric huygens' transmit-arrays as 120 GHz band beamformers. IEEE Access. 2020;8:153815–25. https://doi.org/10.1109/ACCESS.2020.3018297.
39. Lamminen A, Säily J, Ala-Laurinaho J, de Cos J, Ermolov V. Patch antenna and antenna array on multilayer high-frequency PCB for D-band. IEEE Open J Antennas Propag. 2020;1:396–403. https://doi.org/10.1109/OJAP.2020.3004533.

40. Wu GB, Zeng Y-S, Chan KF, Qu S-W, Chan CH. High-gain circularly polarized lens antenna for terahertz applications. IEEE Antennas Wirel Propag Lett. 2019;18(5):921–5. https://doi.org/10.1109/LAWP.2019.2905872.
41. Kumar R, Gupta SK, Wang H-C, Kumari CS, Sai Srinivas Vara Prasad Korlam. From efficiency to sustainability: exploring the potential of 6G for a greener future. Sustainability. 2023;15(23):16387. https://doi.org/10.3390/su152316387.
42. Thornton J, Huang K. Modern lens antennas for communications engineering. Hoboken: Wiley; 2013.
43. Kamruzzaman MM, Trabelsi Y, Nishat H, et al. The smart enhancement of near field sensing range for terahertz antenna in 6G wireless communication systems. Opt Quant Electron. 2024;56:1452. https://doi.org/10.1007/s11082-024-06898-3.
44. Shi E, et al. RIS-aided cell-free massive MIMO systems for 6G: fundamentals, system design, and applications. Proc IEEE. 2024;112(4):331–64. https://doi.org/10.1109/JPROC.2024.3404491.
45. Xu F, Yao J, Lai W, Shen K, Li X, Chen X, Luo ZQ. Coordinating multiple intelligent reflecting surfaces without channel information. IEEE Trans Signal Process. 2024;72:31–46. https://doi.org/10.1109/TSP.2023.3334818.
46. "Antenna theory: analysis and design" by Contantine A. Balanis, 3rd edition. Wiley-Interscience: New York.
47. Li B, Dupleich D, Xia G, Zhou H, Zhang Y, Xiao P, Yang L-L. MDD-enabled two-tier terahertz fronthaul in indoor industrial cell-free massive MIMO. IEEE Trans Commun. 2024;72(3):1653–1670. https://doi.org/10.1109/TCOMM.2023.3330893.
48. Chen Y, Han C, Yu Z, Wang G. Channel measurement, characterization and modeling for terahertz indoor communications above 200 GHz. IEEE Trans Wireless Commun. 2024. https://doi.org/10.1109/twc.2023.3333222.
49. Zheng Y, Wang CX, Yang R, Yu L, Lai F, Huang J, Feng R, Wang C, Li C, Zhong Z. Ultra-massive MIMO channel measurements at 5.3 GHz and a general 6G channel model. IEEE Trans Veh Technol. 2023;72(1):20–34. https://doi.org/10.1109/TVT.2022.3205896.
50. Chafii M, Naoumi S, Alami R, Almazrouei E, Bennis M, Debbah M. Emergent communication in multi-agent reinforcement learning for future wireless networks. IEEE Internet Things Mag. 2023;6(4):18–24. https://doi.org/10.1109/IOTM.001.2300102.